Ultrasonic investigation of critical dynamics in $KMnF_3$

R. M. Holt* and K. Fossheim
Department of Physics, University of Trondheim,
The Norwegian Institute of Technology, 7034 NTH, Trondheim, Norway
(Received 13 November 1980)

An extensive ultrasonic investigation of the cubic-tetragonal phase transition in $KMnF_3$ with respect to temperature, frequency, mode, and sample dependence has been carried out by means of wave-vector-reversed echo technique as well as conventional pulse reflections. All measurements of the attenuation α obey a dynamic scaling law $\alpha \sim \omega^2 t^{-\rho} G(\omega\tau)$. We have measured $\rho = 1.87 \pm 0.05$, in accord with the predictions of the three-dimensional Heisenberg model, a result which is consistent with the expected value $\phi \approx 1.26$ for the anisotropy crossover exponent. The relaxation time τ, governing the dynamics of ordered clusters, is found to be $\approx (9 \times 10^{-13}) t^{-1.41}$ s. The form of the scaling function G is experimentally determined, and its expected limiting forms at low and high $\omega\tau$ values discussed.

I. INTRODUCTION

Ultrasonic methods provide an important probe of critical behavior near structural phase transitions. The critical attenuation and the sound velocity provide information about qualitative or "universal" properties as well as quantitative system dependent features of the transition. Static or dynamic properties may be studied, depending on whether the ultrasonic frequency is lower or higher than the relaxation rate of the critical fluctuations.

The important role of fluctuations in ultrasonic experiments was first established more than ten years ago in $SrTiO_3$.[1] Since then, several experimental investigations have been performed in the perovskite structures. For reasons which were previously not understood, a wide range of critical exponents was observed. One of the motivations for the work presented here was the realization that the sample quality problem could have been one of the main causes of these variations. In an inhomogeneous crystal, where the transition temperature T_c varies slightly with position, i.e., $T_c = T_c(\vec{r})$, the acoustic wave fronts may be severely distorted during propagation due to the strong spatial variation of the sound velocity through the dependence on reduced temperature $t(\vec{r}) = (T - T_c)/T_c$. Such problems may seriously affect the results near T_c. In addition, as we have shown in a recent paper,[2] critical exponents have often been determined from data taken in a temperature region where a simple power law could not be expected, due to the influence of truly dynamical effects, i.e., effects associated with finite $\omega\tau$ values. Here ω is the sound frequency and τ the relaxation time for fluctuations.

In particular, the situation in $KMnF_3$ has been rather unclear. The temperature dependence of the critical attenuation, $\alpha \sim t^{-\rho}$, has been discussed in several papers.[3–6] Fossheim *et al.*[3] found a change in ρ from 1.95 to 1.25 about 1 K above T_c, using an 11.7-MHz longitudinal [100] mode. This effect was interpreted as a possible manifestation of a dimensional crossover. Later extensions of the theory (see Sec. II), however, seemed to exclude this explanation. Domb *et al.*[4] found a temperature independent $\rho \sim 1.3$ from measurements with longitudinal waves along [123]. Courdille and Dumas[5] measured ρ values varying slightly from mode to mode, in the range 1.1–1.4. Recently, Suzuki[6] has obtained a ρ crossing from 1.6 to 1.1 for the longitudinal [100] mode. Concerning the frequency dependence of α, it seems to have been accepted that it deviates from the usual ω^2 law.[3,4,6–8] This was first noticed by Furukawa *et al.*[7] ($\alpha \sim \omega^{1.3}$) and later by Fossheim *et al.*[3] [$\alpha \sim \omega^{n(T)}$, where $n(T) \sim 1.3$–1.4] and Domb *et al.*[4] ($\alpha \sim \omega^{1.2}$). Hatta *et al.*[8] were able to fit their data to a relaxation formula $\alpha \sim C\omega^2\tau_c/(1+\omega^2\tau_c^2)$ where C and τ_c were temperature-dependent parameters. The relaxation time τ_c was related to the central peak width. Suzuki[6] found that the attenuation could be described by a dynamic scaling function. Unfortunately, however, his measurements were carried out in a too-narrow temperature range to include the truly hydrodynamic behavior.

To improve our understanding of the critical features of this and similar structural phase transitions, we found it necessary to perform an extensive investigation of the frequency, temperature, mode, and sample dependence of the attenuation.[2] To this end, and in order to eliminate the sample quality problem, a new technique was developed based on application of wave vector reversed phonon echoes. Since this technique has been presented in more detail elsewhere[9] it will only be briefly sketched here

 ©1981 The American Physical Society

(Sec. III), after a short review of the present theory for ultrasonic absorption near structural transitions (Sec. II). The main topic of the paper, attenuation measurements above T_c in $KMnF_3$, is covered in Secs. IV and V. Some results obtained below T_c are given in Sec. VI. Concluding remarks are presented in Sec. VII.

II. THEORY

At 187 K, $KMnF_3$ undergoes a weakly first-order transition from a cubic (O_h^1) to a tetragonal (D_{4h}^{18}) phase. The order parameter is the rotation angle of MnF_6 octahedra, and the transition is driven by a soft optic mode at the R corner of the Brillouin zone. The first-order nature of the transition is believed to be caused by critical fluctuations via the anisotropic dispersion of the soft mode.[10] It is unclear whether the system is described by a Heisenberg (HFP) or a cubic (CFP) fixed point, but it is generally believed to belong to a universality class with space and spin dimensionalities $d=n=3$. However, the strongly two-dimensional fluctuation correlations have led to the idea[11] that a dimensional crossover might be observable.[3]

Following Aharony,[12] we write the coupling part of the Feder-Pytte Hamiltonian in the following way:

$$H=\int d^dr\Bigg[B_1\sum_{\alpha=1}^{n}S_{\alpha\alpha}[Q_\alpha(\vec{r})]^2 + B_2\sum_{\alpha=1}^{n}S_{\alpha\alpha}[nQ_\alpha^2(\vec{r})-Q^2(\vec{r})] + B_3\sum_{\alpha\neq\beta}S_{\alpha\beta}Q_\alpha(\vec{r})Q_\beta(\vec{r})\Bigg] \quad . \tag{1}$$

Here $Q_\alpha(\vec{r})$ is the α component of the local rotation angle, while the $S_{\alpha\beta}$ are mechanical strain components. The coupling constants B_j are assumed to be only weakly temperature dependent. While the effect of the B_1 term is simply to shift the transition temperature, the B_2 and B_3 terms correspond to interactions in analogy with anisotropic exchange interactions in magnetic systems, leading to crossover exponents ϕ_2 and ϕ_3.[13,14] For instance, as can be seen directly from Eq. (1), with stress applied along [100], ordering will be preferable $\perp$ [100] when $p>0$ ($B_2>0$, XY model), and $\parallel$ [100] when $p<0$ (Ising model). $p=0$ corresponds to the Heisenberg model. ϕ_2 is hence a measure of the relative stability of the corresponding fixed points.

According to Pytte,[15] the ultrasonic absorption in the cubic phase for a mode propagating with wave vector $\vec{k}$ and polarization in the μ direction may be written

$$\alpha(\vec{k},\mu)=\frac{1}{2\omega v(\vec{k},\mu)}\,\mathrm{Im}P(\omega,\vec{k},\mu) \quad , \tag{2}$$

where $P(\omega,\vec{k},\mu)$ is the canonical conjugate momentum to the normal mode coordinate, and $v(\vec{k},\mu)$ is the sound velocity. $P(\omega,\vec{k},\mu)$ may be expressed by four-point time correlation functions

$$\Gamma_{\alpha\beta;\gamma\delta}=\langle Q_\alpha(t)Q_\beta(t)Q_\gamma(t')Q_\delta(t')\rangle \tag{3}$$

and is written

$$P(\omega,\vec{k},\mu)\sim\omega^2D(\omega,\vec{k}) \quad . \tag{4}$$

Here $D(\omega,\vec{k})$ is a linear combination of Fourier transformed correlation functions. For the terms associated with the B_1 part of Eq. (1), the relevant sum of the functions in Eq. (3) may be written as an energy-energy correlation function

$$\sum_{\alpha\beta}\Gamma_{\alpha\alpha;\beta\beta}=\Big\langle\sum_\alpha Q_\alpha(t)Q_\alpha(t)\sum_\beta Q_\beta(t')Q_\beta(t')\Big\rangle \quad . \tag{5}$$

In that case, as is known from dynamic scaling theory[16]

$$D_1(\omega,\vec{k})\sim t^{-(\alpha+\nu z)}G_1(\omega\tau,k\xi) \quad . \tag{6}$$

Here α is the specific-heat exponent, and the dynamic exponent $z=2+(6\ln\frac{4}{3}-1)\eta$ in lowest-order ϵ expansion. ν and η are, respectively, the usual exponents for the temperature and k dependence of the correlations. $G_1(\omega\tau,k\xi)$ is a dynamic scaling function, depending on the correlation length

$$\xi\sim\xi_0t^{-\nu} \tag{7}$$

and on the decay time of the fluctuations

$$\tau\sim\tau_0t^{-\nu z} \quad . \tag{8}$$

The terms arising from the B_2 and B_3 parts of Eq. (1) are derived from correlation functions $\Gamma_{12;12}$ and $\Gamma_{11;11}-\Gamma_{11;22}$, respectively. These are "spin-spin" correlation functions of lower symmetry than those arising from B_1 terms. Since the coupling constants B_2 and B_3 may be considered as analogous to exchange fields, the corresponding correlation functions incorporate the crossover exponents ϕ_2 and ϕ_3 (Ref. 16):

$$D_2(\omega,\vec{k})\sim t^{-[\alpha+\nu z+2(\phi_2-1)]}G_2(\omega\tau,k\xi) \quad , \tag{9}$$

$$D_3(\omega,\vec{k})\sim t^{-[\alpha+\nu z+2(\phi_3-1)]}G_3(\omega\tau,k\xi) \quad . \tag{10}$$

The general expression for the attenuation will hence include up to three terms

$$\alpha_j\sim\omega^2t^{-\rho_j}G_j(\omega\tau,k\xi) \quad , \tag{11}$$

where the critical exponents ρ_j are given as

$$\rho_1=\alpha+\nu z \quad , \tag{12}$$

$$\rho_2=\rho_1+2(\phi_2-1) \quad , \tag{13}$$

$$\rho_3=\rho_1+2(\phi_3-1) \quad . \tag{14}$$

TABLE I. Exponents for critical sound attenuation calculated by second-order ϵ expansion.

$d=3$	ρ_1		ρ_2		ρ_3	
	HFP	CFP	HFP	CFP	HFP	CFP
Ising ($n=1$)	1.39		1.59		1.59	
XY ($n=2$)	1.36	1.39	1.73	1.92	1.73	1.39
Heisenberg ($n=3$)	1.34	1.33	1.86	1.87	1.86	1.84

Here ρ_1 corresponds to the result derived by Kawasaki[17] by means of a mode coupling approach. ϕ_2 and ϕ_3 have been derived by Wilson[18] and Aharony.[19] At the HFP $\phi_2=\phi_3$, while they differ at the CFP. For $d=n=3$, $\phi_2(\text{HFP})=\phi_3(\text{HFP})=1.26$, $\phi_2(\text{CFP})=1.27$, $\phi_3(\text{CFP})=1.26$. In Table I we show the resulting values for ρ_1, ρ_2, and ρ_3 in the three-dimensional case.[20]

Murata[20] calculated the ultrasonic attenuation using the ϵ expansion in renormalization-group theory. He assumed the acoustic wavelength $\lambda=2\pi/k$ to be much larger than the correlation length ξ; i.e., $k\xi \ll 1$. Further, the relaxation time was assumed to be short compared to the period of the sound wave ($\omega\tau \ll 1$). This means that he assumed all scaling functions $G_j(\omega\tau,k\xi)=1$. The resulting absorption is written

$$\alpha(\vec{k},\mu)=\frac{\omega^2}{4M_c k_B T v^3(\vec{k},\mu)} g(\vec{k},\mu) \ , \qquad (15)$$

where the critical part $g(\vec{k},\mu)$ is given for four different modes in Table II.[20] M_c is the unit-cell mass, and $k_B T$ the thermal energy. K_1, K_2, and K_3 in Table II are constants with unknown values, appearing in the calculations of the Fourier transformed correlation functions. The B's and the K's reflect the quantitative (and hence less important) details of the Hamiltonian, while the universal, qualitative features are expressed by the critical exponents ρ_1, ρ_2, and ρ_3 given in Eqs. (12)–(14). Notice however, that there may exist universal ratios between coupling constants.[21]

TABLE II. Sound attenuation functions $g(\vec{k},\mu)$ entering Eq. (15) for four different modes of propagation.

$\vec{k}$	μ	$g(\vec{k},\mu)$
[100]	Longitudinal	g_1+g_2
[110]	Longitudinal	$g_1+\frac{1}{4}g_2+g_3$
[111]	Longitudinal	$g_1+\frac{4}{3}g_3$
[100]	Transversal	g_3

$g_j=K_j B_j^2 t^{-\rho_j}$, $(j=1,2,3)$

As mentioned, Murata's results are valid only in the quasistatic region. Closer to T_c, when τ [Eq. (8)] tends to diverge, the requirement $\omega\tau \ll 1$ may be relaxed. Still, for reasonable acoustic wavelengths, $k\xi \ll 1$ will be assumed to be valid, even very close to T_c. For each of the different terms α_j [Eq. (11)] contributing to α, we thus have to incorporate the corresponding dynamic scaling function $G_j(\omega\tau,k\xi=0)$, as has been pointed out before.[2]

As mentioned, the dynamic scaling hypothesis assumes

$$G_j(\omega\tau)\simeq 1, \quad \text{for } \omega\tau\to 0 \ . \qquad (16)$$

Now, since the critical slowing down is characterized by an infinitely long relaxation time, singularities in the ultrasonic attenuation may only occur at $\omega=0$. Hence, α should be temperature independent in the limit $t\to 0 (T\to T_c)$ for $\omega\neq 0$; i.e., $G_j(\omega\tau)$ should be written

$$G_j(\omega\tau)\sim(\omega\tau)^{-\kappa_j}, \quad \text{for } \omega\tau\to\infty \qquad (17)$$

and the exponents κ_j determined by the condition

$$\alpha_j(t\to 0)\sim\omega^{2-\kappa_j}t^{-(\rho_j-\nu z\kappa_j)}\sim t^0 \ , \qquad (18)$$

which directly gives $\kappa_j=\rho_j/\nu z$, or $\kappa_1=0.94$ and $\kappa_2=\kappa_3=1.32$. Little is known theoretically about the form of G_j in the region between the two limiting values of $\omega\tau$.

III. EXPERIMENTAL METHOD

We have measured ultrasonic attenuation in $KMnF_3$ using the conventional pulse reflection method as well as the novel phonon echo technique.[2,9] In the latter case (see Fig. 1), a sound pulse at frequency ω is transmitted from the sample through an acoustic bond (Nonaq stopcock grease) into an echo active single crystal ($Bi_{12}GeO_{20}$). This crystal is placed in the electric field of a helical resonant cavity, which is tuned[22] to 2ω. A phonon

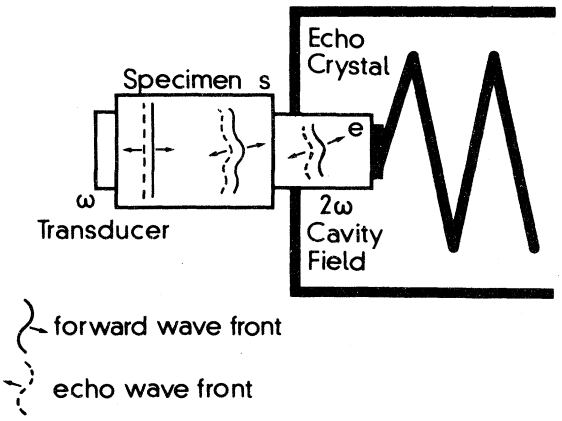

FIG. 1. Experimental setup for phonon echo investigation of a nonechoactive specimen, as for instance $KMnF_3$. The echo crystal is located in a tunable spiral cavity.

echo results from the bilinear interaction between the field $E = E_0 e^{j2\omega t}$ and the initial sound wave $S = S_0 e^{-j(\omega t - \vec{k}\cdot\vec{r})}$. The echo may be written

$$e \sim \gamma S_0 E_0 e^{j(\omega t + \vec{k}\cdot\vec{r})} \quad . \tag{19}$$

γ is a material parameter characterizing the echo generation efficiency. This effect was first seen by Thompson and Quate[23] in $LiNbO_3$. A possible interpretation of Eq. (19) is that even in case of a distorted wave front the echo wave vector is reversed at every point of the wave front during echo generation. Hence the echo propagates backward such that its wave front reconstructs continuously into that of the initial wave. This means that there will always be constructive interference at the detecting ($LiNbO_3$) transducer. Consequently, the problem of low acoustic sample quality has been considerably reduced. With a small and nearly temperature-independent attenuation constant near 187 K in $Bi_{12}GeO_{20}$, the temperature dependence of the echo amplitude directly gives the critical absorption in $KMnF_3$.

Measurements with the echo technique could be performed in the frequency range 60–250 MHz using tunable spiral cavities. In the present experiments, transducer efficiency and bond losses set the upper frequency limit, while the lower limit was due to the tuning range of the cavities. This is however, merely a practical limitation. Echoes may be used below this frequency range by replacing the cavities with resonant LC circuits, and above by using evaporated-thin-film transducers. Reflected pulse data could also be taken simultaneously with echo data, and far away from T_c these were shown to agree. We have measured the attenuation for four different modes (longitudinal waves along [100], [110], and [111], transversal waves along [100]) using four different samples up to ~ 50 K above T_c and throughout the frequency region 15–700 MHz. Above 250 MHz conventional technique was employed.

Crystals from two different sources have been used (see Table III). Samples I–III were grown from melt in He atmosphere by Dr. A. Linz at the Crystal Physics Laboratory of MIT around 1970. The quality of the samples then was extremely good, as was shown by neutron scattering.[3] Some of them (especially II) were later exposed to mechanical stress which had introduced considerable defects. Sample IV was cut from a sphere grown by CEN in Grenoble in 1979.

For temperature control a Linear Research LR-130 unit was used along with an LR-110 Resistance Bridge for temperature measurements. Homemade Cu wire thermometers as well as commercial Rosemount Inc. Pt thermometers were used throughout the experiments. The reproducibility of both was checked to be within the temperature resolution (~ 0.01 K) of our experiments. All data were taken as a function of decreasing temperature at constant frequency. The temperature was controlled and stabilized within ~ 2 mK, using a stabilization time of ~ 10–20 min per measurement. Care was taken to avoid heating of the sample by the power of the acoustic pulses. It was also checked that reflection and echo amplitudes varied linearly with input signal strength.

The critical part of the attenuation was obtained by subtracting a very weakly temperature-dependent background. The background level was estimated from least-squares calculations, but could not be

TABLE III. $KMnF_3$ samples used in the present work. $T_m (\approx T_c)$ is the temperature of maximum attenuation at low frequency (measured with decreasing temperature).

Sample No.	I	II	III	IV
Orientation	[110]	[100]/[110]	[111]	[110]
Length $2L$ (cm)	1.75	1.67/1.44	1.49	2.09
Acoustic quality	Good	Poor	Good	Very good
Origin	MIT, 1970	MIT, 1970	MIT, 1970	CEN, 1979
Measured T_m(K)	187.20	187.12	187.21	187.15

determined more accurately than within ± 0.5 dB/$2L$ (L being the length of sample). Because of the weak first-order character of the transition, the results could be analyzed as a function of $\Delta T = T - T_m \approx T - T_c$ where T_m is the temperature of maximum attenuation at low frequency. A thermal hysteresis ranging from $\lesssim 0.02$ K (samples I–III) to 0.12 K (sample IV) was observed. Hence, at least for data taken more than 1 K above T_c, this does not affect the measured exponents ρ significantly.

IV. MEASUREMENTS ABOVE T_c

A. Longitudinal waves, $\vec{k} \| [100]$

Experiments with longitudinally polarized waves along [100] were performed in samples I and II (see Table III).

Attenuation data obtained in I are presented as a function of the temperature deviation ΔT in Fig. 2 and as a function of frequency in Fig. 3. Only in a temperature range several degrees above T_c do the measurements confirm a law like Eq. (15), with the frequency dependence ω^2 expected from the Murata theory. When the linear parts of curves like those in Fig. 2 are analyzed by least-squares fits for 11 different frequencies, the exponent $\rho = 1.87 \pm 0.04$ results. Hence, for $\Delta T \gtrsim 7$ K, α can be expressed as

$$\alpha \sim \omega^{2.0 \pm 0.1} t^{-1.87 \pm 0.04} . \qquad (20)$$

Thus, our results indicate that g_2 (Table II) dominates over g_1 in the expression for α with $\vec{k} \| [100]$,

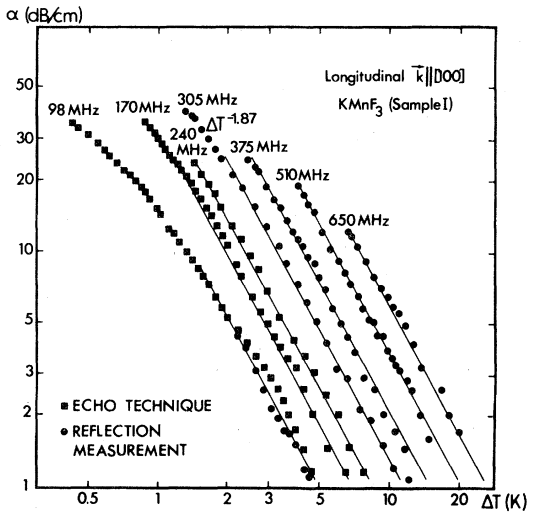

FIG. 2. Temperature dependence of the critical attenuation of the longitudinal [100] mode in $KMnF_3$ (sample I), with the expected $t^{-1.87}$ law shown at each frequency. The uncertainty in determination of the background level was here, as well as in the following figures, ± 0.5 dB/cm, and the uncertainty of measurement at each point $\sim \pm 0.2$ dB/cm.

and that the three-dimensional Heisenberg model, for which $\rho_2 = 1.86$ or 1.87 (Table I) governs the behavior of the critical attenuation, at least well above T_c.

On approaching the critical point, on the other hand, we find that the temperature exponent changes to an apparent value of 1.2–1.3. The frequency exponent at the same time crosses gradually over to a

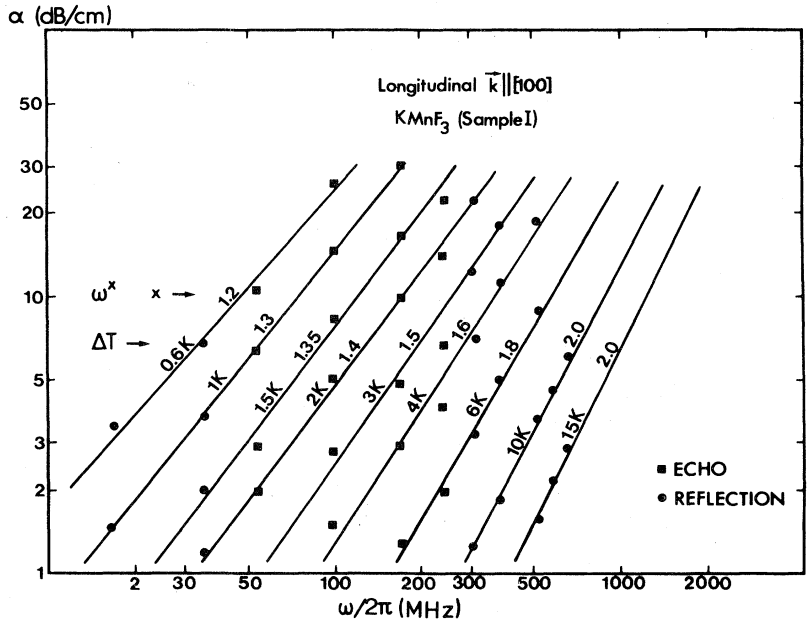

FIG. 3. Frequency dependence of the critical attenuation of the longitudinal [100] mode in $KMnF_3$ (sample I). Straight lines fitted to the data points are shown at each temperature.

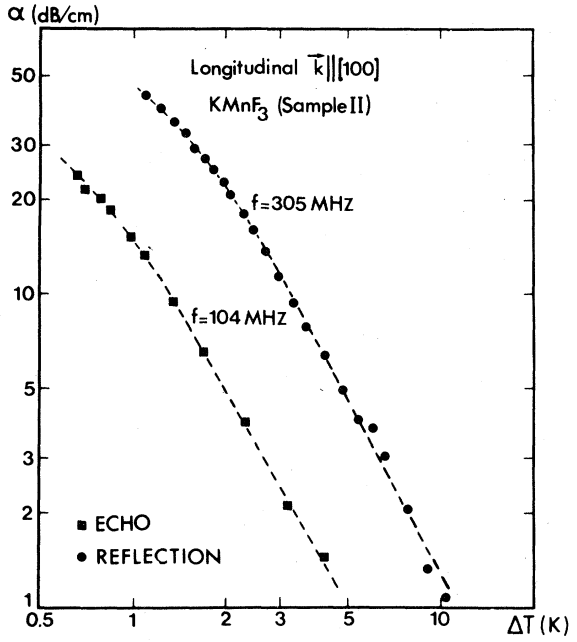

FIG. 4. Measurements of longitudinal attenuation along [100] in sample II compared with the observed behavior in sample I (broken lines).

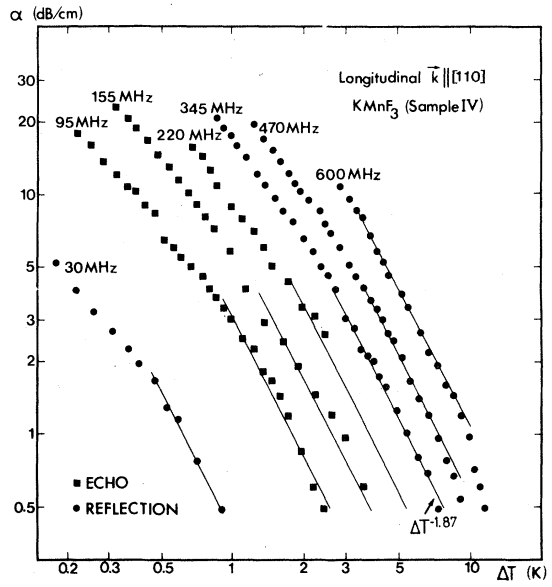

FIG. 5. Temperature dependence of longitudinal attenuation along [110] in $KMnF_3$ (sample IV), with the $t^{-1.87}$ law shown at each frequency.

value of ~ 1.2 about 1 K from T_c. A discussion of this behavior will be given in the next section. Measurements in the close vicinity of T_c were prevented by the large critical attenuation.

Measurements in sample II are shown in Fig. 4. Comparison with sample I, shows that, at least for $\Delta T \gtrsim 0.7$ K, crystals of the same origin, but with different content of internal strains, behave similarly both with respect to critical exponent and the quantitative features reflected by the absolute value of α.

B. Longitudinal waves, $\vec{k} \| [110]$

Experiments have been performed with samples II and IV using longitudinal waves propagating along [110]. Data could be taken much closer to T_c here than in the case above, since α was much lower.

For sample II, the trend in both temperature and frequency dependence is the same as in the [100] direction. Far from T_c, $\rho = 1.8 \pm 0.1$, and the frequency dependence also approaches a ω^2 law. However, close to T_c, the temperature dependence changes in a somewhat shoulder-like fashion, a fact which may partly be due to defects. We recall here from Table III that sample II is of rather poor quality.

Hence, in order to compare two crystals of different origin, experiments with $\vec{k} \| [110]$ were also done in sample IV, which was of extremely high acoustic quality. Data are given in Figs. 5 and 6, and the result is $\rho = 1.86 \pm 0.15$, obtained from least-squares fits for the seven different frequencies used, well above T_c. Close to T_c, on the other hand, the exponent crosses smoothly to a value $\rho \sim 1.2$–1.3, i.e., the same as for $\vec{k} \| [100]$. Hence, we are allowed to conclude that in spite of the agreement well above T_c the behavior in the near vicinity of the critical point is different for crystals II and IV. This is probably due to internal strains in sample II. However,

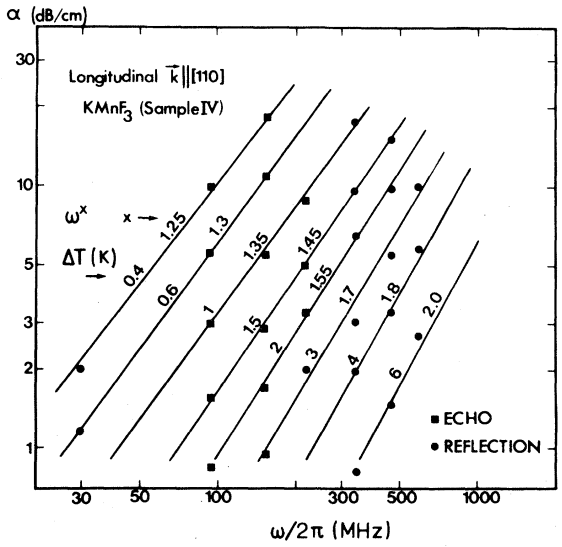

FIG. 6. Frequency dependence of the longitudinal attenuation along [110] in $KMnF_3$ (sample IV). Fitted lines through the data points are shown at each temperature.

impurities may also be of importance here. Since no theoretical treatment of the role of defects exists for ultrasonic attenuation near a structural phase transition, we shall not discuss this point any further.

It is clear however, and of great importance, that the *qualitative* features as expressed by the value of the exponent ρ and the frequency dependence $\alpha \sim \omega^2$ far from T_c, are independent of sample quality and origin. The absolute value of α turns out to be ~ 20–30% larger in crystal II than in IV. This means that the *quantitative* features of the transition are sample dependent, as one could expect. Bearing in mind that $\alpha(\mathrm{I}) = \alpha(\mathrm{II})$ (I and II are of the same origin) for $\vec{k} \| [100]$, this sample dependence between II and IV may be connected to the difference in impurity content of the two crystals from different sources.

C. Transversal waves, $\vec{k} \| [100]$

Shear-wave experiments were done in sample I. Transmission of shear waves through the acoustic bond was much lower than that of longitudinal waves, and echo experiments could be performed only in one case (at 150 MHz). The measurements indicate (see Fig. 7) the value $\rho = 1.90 \pm 0.10$ far from T_c.

From Table II one finds that the critical attenuation for this mode is described by only one term, namely, g_3. Thus we have determined $\rho_3 = 1.9 \pm 0.1$, in agreement with the three-dimensional Heisenberg model. It is not possible within our limits of uncertainty to distinguish between the Heisenberg and cubic fixed points.

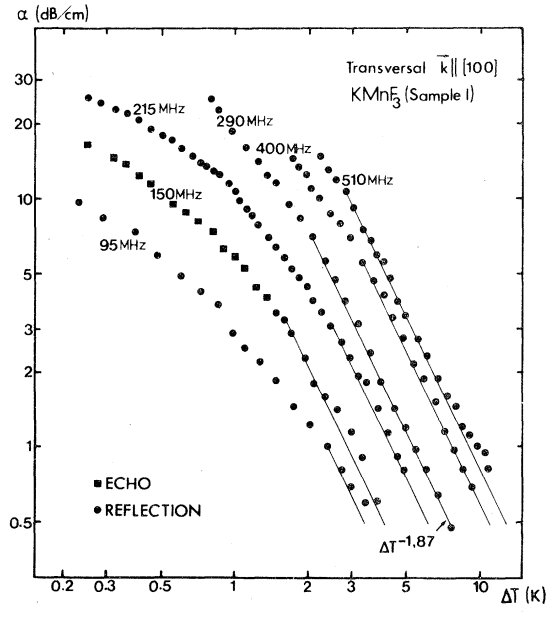

FIG. 7. Temperature dependence of transversal attenuation along [100] in $KMnF_3$ (sample I), with the $t^{-1.87}$ law shown at each frequency.

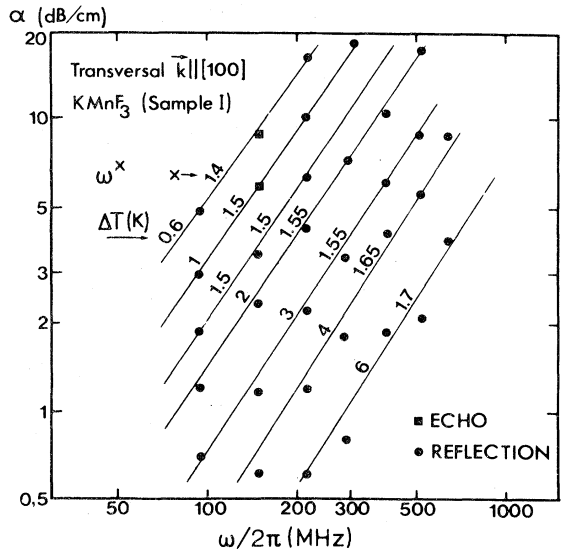

FIG. 8. Frequency dependence of transversal attenuation along [100] in $KMnF_3$ (sample I). Straight lines fitted to the data points are shown at each temperature.

A change in frequency dependence similar to that for the other modes is also found (see Fig. 8).

D. Longitudinal waves, $\vec{k} \| [111]$

Sample III, of the same source as samples I and II, was used in our experiments with longitudinal waves propagating along [111]. Data are given in Figs. 9 and 10. The most remarkable feature is the extremely low attenuation. At 100 MHz and 1 K from the transition we find an attenuation only $\sim \frac{1}{20}$ of α for longitudinal L[100] and $\sim \frac{1}{4}$ of α for transversal waves T[100] in the [100] direction, measured on the logarithmic dB scale. This of course leads to comparatively large uncertainties in determination of the behavior far from T_c, where we expect to measure the true value of the critical exponent ρ. Below 200 MHz, all measurements are clearly in the region where rounding of the exponent occurs. At frequencies above 200 MHz, ρ seems to be 1.80 ± 0.15. This is significantly larger than the value of $\rho_1 = 1.34$ in Murata's theory, which predicts that the attenuation of this mode is given by a superposition of g_1 and g_3. Hence the experiments indicate that g_3 dominates the picture. The frequency dependence (Fig. 10) changes slowly with temperature, in a manner similar to that seen for the other modes investigated.

For this mode we also measured the sound velocity versus temperature (Fig. 11), using the pulse overlap technique.[24] According to Murata[20] the critical part of the velocity may be expressed similarly to the critical attenuation (Table II), but with constants L_j re-

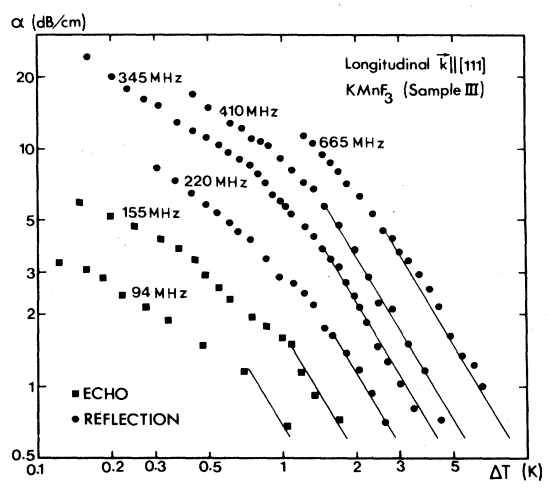

FIG. 9. Temperature dependence of longitudinal attenuation along [111] in $KMnF_3$ (sample III), with the $t^{-1.87}$ law shown for comparison by a straight line at each frequency far from T_c.

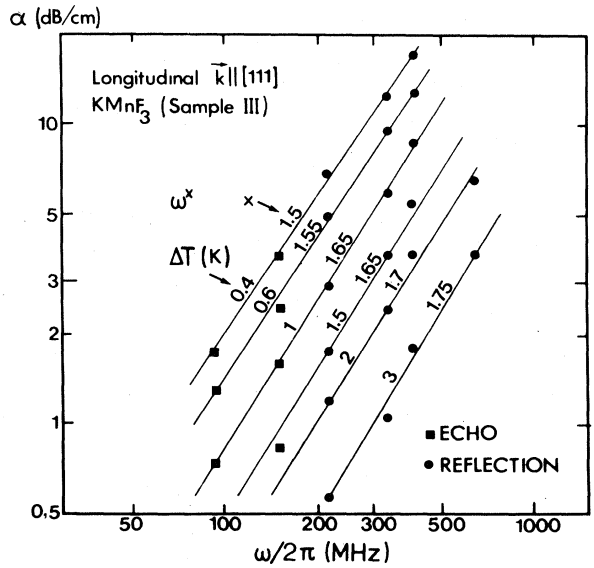

FIG. 10. Frequency dependence of longitudinal attenuation along [111] in $KMnF_3$ (sample III). Straight lines fitted to the data points are shown at each temperature.

placing K_j and with critical exponents $\mu_1 = \alpha$ (specific-heat exponent), $\mu_3 = \mu_1 + 2(\phi_3 - 1)$. From the insert in Fig. 11 we see that in the region corresponding to $\alpha \sim \omega^2 t^{-1.86}$ we find $\mu = 0.4 \pm 0.1$, in agreement with the expected value[14] for μ_3. This may indicate, however, being far from a proof, that g_3 really is the leading term in the attenuation of the L[111] mode. The rounding closer to T_c is presumably of dynamic origin similar to what is found for the attenuation (see Sec. V). The behavior at $\Delta T > 10$ K where μ crosses to ~ 0.9–1 is not understood. We recall, however, that similar observations have been made before[25,26] for the L[100] mode.

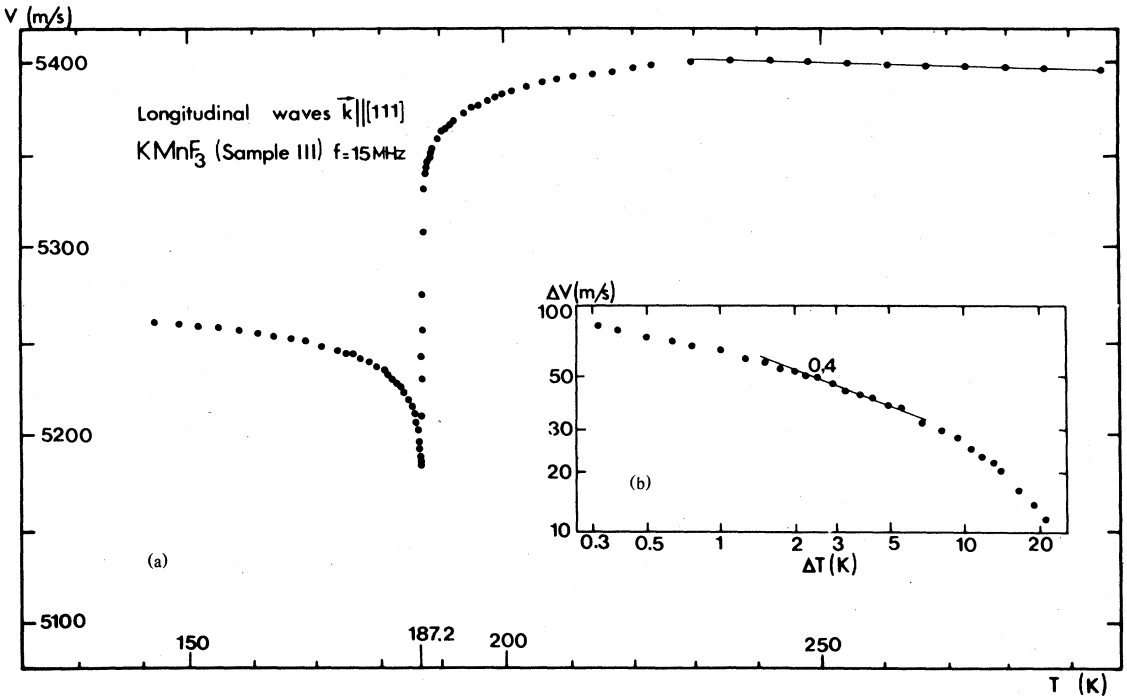

FIG. 11. Temperature dependence of sound velocity for the longitudinal [111] mode in $KMnF_3$ (sample III). In (a) the fully drawn line represents the weakly temperature dependent background which is subtracted when the log-log plot in (b) is drawn.

V. DISCUSSION OF THE RESULTS ABOVE T_c

We are now, from the data presented in the preceding section, in position to estimate numerically the weight of g_1, g_2, and g_3 relative to each other. To do that, the data must be scaled with the third power of the measured sound velocity v in the respective directions [recall Eq. (15)]. Having data for four different modes, we have an overdetermined system of equations in the three unknown parameters $K_1B_1^2$, $K_2B_2^2$, and $K_3B_3^2$ here represented by g_1, g_2, and g_3 (see Table II). We have seen, however, that the absolute value of α depends upon the origin of the sample. Therefore we use only the data for samples I, II, and III (for $T > 7$ K) and give only ratios between the coupling constants. We deduce the following:

$$\left|\left(\frac{K_2}{K_3}\right)^{1/2}\frac{B_2}{B_3}\right| = 7.2 \pm 0.3 \ , \tag{21}$$

$$\left|\left(\frac{K_1}{K_3}\right)^{1/2}\frac{B_1}{B_3}\right| = 0.75 \pm 0.3 \ . \tag{22}$$

Data for all modes are consistent with these values, within the limits of uncertainty. Notice that even if the exponent ρ_1 never can be measured directly, it is still possible to estimate the weight of the term g_1 in comparison with g_2 and g_3.

To summarize, we have seen that the critical attentuation far from T_c behaves according to Murata's[20] and Schwabl's[21] predictions for the hydrodynamic regime, i.e., $\alpha \sim \omega^2 t^{-\rho}$ with $\rho = 1.87 \pm 0.05$, for all modes investigated. This is the value expected for a three-dimensional Heisenberg model, which is believed to describe the critical features of the cubic perovskites. The results are also consistent with the theoretical value of the anisotropy crossover exponent $\phi \approx 1.26$.

We now turn to a discussion of the behavior closer to T_c. As was seen in Sec. II, we have to incorporate a dynamic scaling function [Eq. (11)] of which we only have some knowledge about the limiting forms [Eqs. (16) and (17)]. From this we can say that the temperature T_Δ at which α_j crosses from a behavior characterized by the theoretically predicted values of the exponents ρ_j to a nonhydrodynamic behavior, is given approximately by

$$\omega\tau = 1 \tag{23}$$

corresponding to

$$t_\Delta = \left(\frac{\omega}{\omega_0}\right)^{1/\nu z} \ , \tag{24}$$

when Eq. (8) is applied. ω_0 is a constant frequency. Figure 12 shows a log-log plot for the longitudinal [110] mode in sample IV, from which

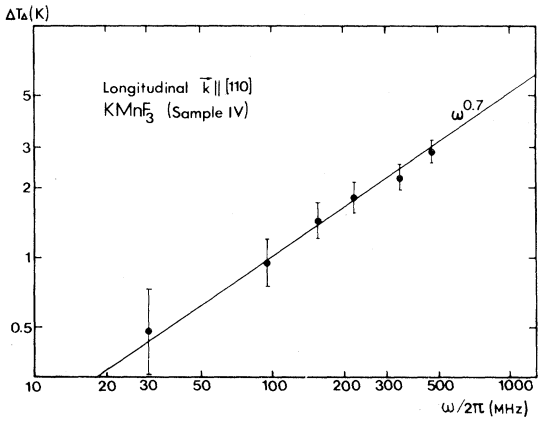

FIG. 12. The temperature ΔT_Δ, at which the "crossover" from Murata's hydrodynamic law occurs, vs frequency for the L[110] mode in sample IV. An $\omega^{0.7}$ law, as expected from dynamic scaling theory, is shown. With an interpretation in terms of cluster dynamics, as suggested in the text, the half width of the central peak may be read, as a function of temperature, from the drawn line.

$$t_\Delta = \left(\frac{\omega}{\omega_0}\right)^{0.70 \pm 0.05} \tag{25}$$

is found, with $\omega_0/2\pi = 1.8 \pm 0.2 \times 10^{11}$ s^{-1}. For the three-dimensional Heisenberg model $1/\nu z = 0.71$. It turns out that for all investigated modes in *all* samples the variation of ΔT_Δ vs ω follows the line in Fig. 12, within limits of uncertainty, but with a greater spread of data points for the other modes.

Rounding, similar to what is seen in the plots of α vs T, often takes place in experimental studies near phase transitions as a result of low sample quality. We have seen, however, in this case that the behavior is systematic in frequency, and sample independent. This is seen by echo technique as well as reflection technique. It should also be clear that the first-order nature of the transition cannot explain the observed change in frequency exponent on approaching T_c. This exponent has a definite value at a fixed temperature, independent of the location of T_c. We thus conclude that the observed deviations from the $\omega^2 t^{-\rho}$ law are due to breakdown of the hydrodynamic approximation $\omega\tau << 1$.

To get a better idea of the form of $G(\omega\tau)$, we have made scaling plots of $\alpha_{obs}/\alpha_0\omega^2 t^{-\rho}$ vs $(\omega\tau)^{-1}$, recalling here that $\alpha_0\omega^2 t^{-\rho}$ is the linear extrapolation of the detected behavior far from T_c. Figure 13 shows the results for the longitudinal [110] mode. The drawn curve is the average for *all* frequencies and *all* modes. There is no significant difference between different samples or different modes. Hence we are allowed to conclude from experiment, that $G_2 \approx G_3$, since α_2(or g_2) and α_3(or g_3) dominate the

critical attenuation for the observed modes. The number of data points and their accuracy at large $\omega\tau$ values are not sufficient to draw any definite conclusions about the limiting form of $G_j(\omega\tau)$. However, the theoretically expected value for $\kappa_2 \approx \kappa_3 \approx 1.32$ [Eq. (18) and following] lies within the limits of experimental uncertainty. We notice also that Fig. 13 may be drawn without the knowledge of Fig. 12, which only gives a numerical scaling factor (ω_0) for the abscissa in Fig. 13.

Some remarks on the physical mechanisms leading to the observed hydrodynamic crossover are in order here. The measured relaxation time (in s)

$$\tau = \frac{1}{\omega_0} t^{-\nu z} \approx 9 \times 10^{-13} t^{-\nu z} \tag{26}$$

is $\sim 1.4 \times 10^{-9}$ s at $\Delta T = 1$ K. From the neutron data of Shapiro *et al.*,[27] the inverse width of the heavily overdamped soft mode in $KMnF_3$ is estimated to be $\sim 10^{-11}$ s close to T_c. The observed relaxation process is thus much too slow to be associated with the soft phonon. The temperature dependence is also quite different, since the width as well as the frequency of the soft mode is almost insensitive to temperature near T_c.

However, in $KMnF_3$ above T_c, persistent Raman scattering has been seen from modes which by symmetry are Raman inactive in the high-temperature phase.[28,29] This indicates a fluctuation induced precursor order due to formation of clusters of the low-temperature phase above T_c. We interpret the relaxation time in Eq. (26) as the lifetime of such correlated regions. At least in the model of Schneider and Stoll,[30] the cluster dynamics is responsible for the central mode phenomenon. A narrow central peak in $KMnF_3$ was found by Shapiro *et al.*[27] Their instrument resolution did not allow any investigation of the peak width which was stated to be $< 4.8 \times 10^9$ s^{-1}. Hence, τ may be interpreted as the inverse width of the central mode. In that case, since $\omega\tau \approx 1$ along the line in Fig. 12, the half width $\Gamma = 1/2\tau$ may be read directly from this figure.

As mentioned in the Introduction, Hatta *et al.*[8] derived a relaxation time τ_c from their measurements of the frequency dependence of α and interpreted it as representing the inverse width of the central mode. They did not obtain a functional form for τ vs ΔT, but found $\tau \sim 4.1 \times 10^{-9}$ s at $\Delta T \sim 0.8$ K and $\tau \sim 0.45 \times 10^{-9}$ s at $\Delta T \sim 4$ K. This is slightly larger, but within the same range as found here. We note that the full temperature dependence for the characteristic time τ was obtained here only by assuming dynamic scaling to be valid. Our results are sample independent within error limits, which indicates that

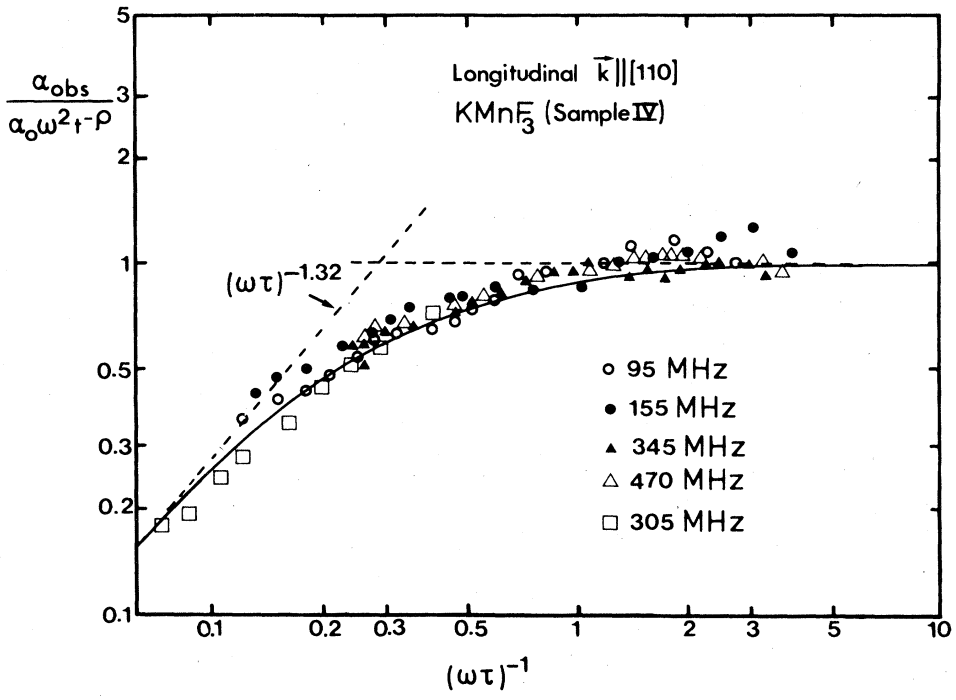

FIG. 13. Scaling plot of observed attenuation vs $(\omega\tau)^{-1}$, where τ is given by Eq. (26). The fully drawn curve is the average over *all* samples, *all* modes, and *all* frequencies. Data points for the [110] mode are shown. Uncertainties of measurements are indicated. Data have not been corrected for the temperature dependence of the sound velocities, which would only cause changes within the limits of uncertainties.

the behavior may be intrinsic. However, no definite conclusions regarding this point can be drawn from measurements on only two samples with unknown concentrations of impurities.

Comparing with other previous work on $KMnF_3$ our results are similar to those obtained by Fossheim *et al.*,[3] particularly with regard to the exponent $\rho = 1.95$, crossing over to a lower value near T_c. However, the conclusions are different, partly due to improved knowledge of the values of critical exponents revealed by the renormalization-group theory. The dependence of ΔT_Δ on ω (Fig. 12) convincingly demonstrates that the change in ρ cannot be due to a dimensional crossover, in which case ΔT_Δ should be insensitive to frequency.

Our results do not agree with those obtained by Domb *et al.*[4] or Courdille and Dumas.[5] In the first case, $\rho = 1.3$ was found for the quasilongitudinal [123] mode. It may well be that the term g_1 with an exponent $\rho_1 = 1.34$ dominates the attenuation in this direction, where no theoretical results are available. It may also be that the data in their investigations to a large extent were taken in the nonhydrodynamic region. However, this question remains since the frequency dependence was not investigated in detail in either of those investigations.

Suzuki[6] analyzed his results in the light of dynamic scaling theory, but did not obtain internal consistency in his data. We believe that this may be caused by having taken measurements in too narrow temperature and frequency regions to permit a complete test of the scaling assumption.

VI. MEASUREMENTS BELOW T_c

While the attenuation above T_c is determined completely by interactions with critical fluctuations and clusters of the ordered phase, the situation below T_c is much more complicated. A sound wave will experience, in addition to fluctuations and clusters of the high-temperature phase, also interactions with the domain walls, either by inelastic damping or elastic scattering. Further, Landau-Khalatnikov damping[31,32] also takes place, with a relaxation time related to the order-parameter dynamics. The resulting acoustic attenuation below T_c is thus much larger than above. This caused all acoustic signals above ~ 100 MHz in our experiments to be completely damped out near and below the critical point for all modes except longitudinal waves along [111]. The small critical attenuation in this direction permitted echo measurements to be done throughout the whole critical region at 94 MHz (Fig. 14). At 155 MHz, the echo vanished in a region narrower than 0.2 K below T_c, where the first reflected pulse still could be detected. All data were taken as function of decreasing temperature with a least interval of 12 mK between the points, and the same stability as before.

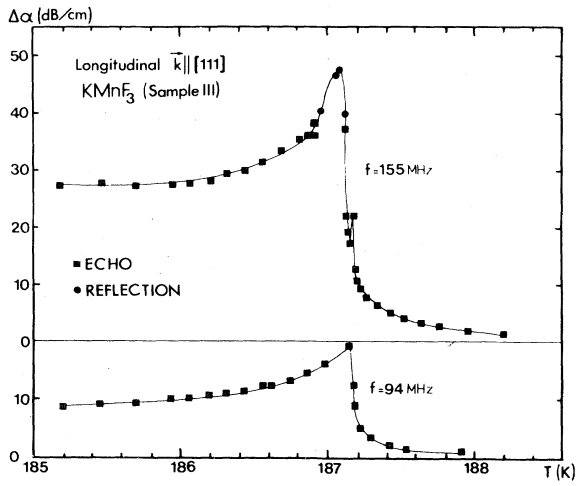

FIG. 14. Longitudinal attenuation [111] above and below T_c in $KMnF_3$ (sample III), measured with echo technique at 94 and 155 MHz. Reflection data are shown near the maximum of the 155 MHz curve where echo data could not be taken. T_c for this sample is ≈ 187.21 K.

During the experiment, echo and reflection measurements were compared in the region below T_c. No significant difference was found, except in the close vicinity of T_c. Hence, we are led to believe that the sound wave interacts with the domain structure and the order parameter mainly via relaxation. If, on the contrary, scattering on domain walls were a primary source of damping, reflections should be more affected than the echo, which is not sensitive to elastic scattering processes, except for possible mode conversion.

The most interesting feature of Fig. 14 is the frequency dependence of the temperature of maximum attenuation. In fact, at 155 MHz, *two* maxima are seen. This behavior may be explained by taking into account a Landau-Khalatnikov form:

$$\alpha_{LK} = \frac{\Delta v}{v^2} \frac{\omega^2 \tau}{1 + \omega^2 \tau^2} \quad . \tag{27}$$

Here Δv is the difference between the sound velocities at $\omega\tau = \infty$ and $\omega\tau = 0$. τ is a temperature-dependent relaxation time

$$\tau = \tau_0 (-t)^{-\nu z} \quad . \tag{28}$$

Hence α_{LK}, which is zero at $t = 0$, peaks at $\omega\tau = 1$. A double maximum like that at 155 MHz may result from superposition of the critical attenuation (centered at $t = 0$) and an LK term [Eq. (27)]. The displacement of the LK-associated maximum from 94 to 155 MHz is $\sim 0.05 \pm 0.015$ K. Curve fitting of the measurements, including 15 MHz reflection data not shown in Fig. 14, gave $\tau \sim (4 \times 10^{-14}) |t|^{-\nu z}$ or $\sim 6 \times 10^{-11}$ s at 1 K below T_c.

We interpret this as the relaxation time of the order parameter. Domain relaxation may be expected to be much slower. In $SrTiO_3$, Fossheim and Berre[33] found $\tau_{\text{domains}} \sim 4 \times 10^{-7}$ s 1 K below T_c. We stress, however, that improved temperature resolution and measurements at more frequencies are necessary to obtain the quantitatively correct relaxation time.

VII. CONCLUSIONS

We draw the following conclusions about the critical behavior in $KMnF_3$ from our experiments with echo and reflection techniques.

Far above T_c, the critical exponent dominating the ultrasonic attenuation is $\rho = 1.87 \pm 0.05$. In this region, the frequency dependence is in accord with an ω^2 law. This is concluded from experiments with four different modes of sound propagation. Samples with different strain and impurity content were used. The behavior agrees with the expected fluctuation dominated attenuation in a three-dimensional Heisenberg system. Thus, the theoretical value $\phi \approx 1.26$ for the anisotropy crossover exponent is confirmed.

The absolute value of the critical attenuation varies slightly between samples of different origin, indicating a dependence on impurities. For samples from one source, the attenuation level for the four modes investigated are found to be consistent with theory. Ratios between the relevant coupling constants are estimated.

On approaching T_c, the apparent exponents for the frequency- and temperature dependence of the attenuation are gradually lowered. The results obey a dynamic scaling law $\alpha \sim \omega^2 t^{-\rho} G(\omega\tau)$ where the frequency and temperature exponents are those determined well above T_c. We have experimentally determined the form of the scaling function G. The measured relaxation time $\tau \approx 9 \times 10^{-13}\ t^{-\nu z}$ s is interpreted as the lifetime of ordered clusters known to exist above T_c. In at least one model this τ gives directly the inverse width of the central mode.

Measurements below T_c with longitudinal waves along [111] indicate order-parameter relaxation of the Landau-Khalatnikov type.

ACKNOWLEDGMENTS

The authors would like to acknowledge illuminating discussions with E. Pytte. NTH's Fund and NAVF (The Norwegian Council for Science and the Humanities) have given financial support to the project.

---

*Present address: Electronics Research Laboratory, University of Trondheim, The Norwegian Institute of Technology, 7034-NTH Trondheim, Norway.

[1]B. Berre, K. Fossheim, and K. A. Müller, Phys. Rev. Lett. 23, 589 (1969).

[2]K. Fossheim and R. M. Holt, Phys. Rev. Lett. 45, 730 (1980).

[3]K. Fossheim, D. Martinsen, and A. Linz, in *Anharmonic Lattices, Structural Transitions and Melting,* edited by T. Riste (Noordhoff, Groningen, 1974), p. 141.

[4]E. R. Domb, H. K. Schurmann, and T. Mihalisin, Phys. Rev. Lett. 36, 1191 (1976).

[5]J. M. Courdille and J. Dumas, Solid State Commun. 9, 609 (1971).

[6]M. Suzuki, J. Phys. C 13, 549 (1980).

[7]M. Furukawa, Y. Fujimori, and K. Hirakawa, J. Phys. Soc. Jpn. 29, 1528 (1970).

[8]I. Hatta, M. Matsuda, and S. Sawada, J. Phys. C 7, 2038 (1973).

[9]R. M. Holt and K. Fossheim, Ferroelectrics 25, 515 (1980); K. Fossheim and R. M. Holt, in *Phonon Scattering in Condensed Matter,* edited by H. J. Maris (Plenum, New York, 1980), p. 291; Physical Acoustics (in press).

[10]A. Aharony, Ferroelectrics 24, 313 (1980).

[11]F. Schwabl, Phys. Rev. B 7, 2038 (1973).

[12]A. Aharony, Ann. Israel Phys. Soc. 2, 13 (1978).

[13]E. K. Riedel and F. Wegner, Z. Phys. 225, 195 (1969); M. E. Fisher, Rev. Mod. Phys. 46, 597 (1974).

[14]A. Aharony and A. D. Bruce, Phys. Rev. Lett. 33, 427 (1974); A. D. Bruce and A. Aharony, Phys. Rev. B 11, 478 (1975).

[15]E. Pytte, Phys. Rev. B 1, 924 (1970).

[16]P. C. Hohenberg and B. I. Halperin, Rev. Mod. Phys. 49, 435 (1977).

[17]K. Kawasaki, in *Internal Friction and Ultrasonic Attenuation in Solids,* edited by R. R. Hasiguti and N. Mikoshiba (University of Tokyo Press, Tokyo, 1977), p. 29.

[18]K. G. Wilson, Phys. Rev. Lett. 28, 548 (1972).

[19]A. Aharony, Phys. Lett. A 49, 221 (1974).

[20]K. K. Murata, Phys. Rev. B 13, 4015 (1976); F. Schwabl (private communication) has verified Murata's calculations using a mode-mode coupling approach. The numerical coefficients quoted here are as given by Schwabl.

[21]A. Aharony and P. C. Hohenberg, Phys. Rev. B 13, 3081 (1976).

[22]K. Fossheim and R. M. Holt, J. Phys. E 11, 892 (1978).

[23]R. B. Thompson and C. F. Quate, Appl. Phys. Lett. 16, 295 (1970). For a technical demonstration of echo properties, see also for instance N. S. Shiren and R. L. Melcher [1974 Ultrasonics Symposium Proceedings, IEEE Catalog No. 74CH 896-ISU, p. 558 and *Phonon Scattering in Solids,* edited by L. J. Challis, V. W. Rampton, and A. F. G. Wyatt (Plenum, New York, 1975), p. 405].

[24]E. P. Papadakis, J. Acoust. Soc. Am. 42, 1045 (1967).

[25]R. L. Melcher and R. H. Plovnick, in *Phonons,* edited by M. A. Nusimovici (Flammarion, Paris, 1971), p. 348.

[26]M. Matsuda, I. Hatta, and S. Sawada, Ferroelectrics 8, 595 (1974).

[27]S. M. Shapiro, J. D. Axe, G. Shirane, and T. Riste, Phys. Rev. B 6, 4332 (1972).
[28]D. J. Lockwood and B. H. Torrie, in *Anharmonic Lattices, Structural Transitions and Melting,* edited by T. Riste (Noordhoff, Groningen, 1974), p. 147.
[29]A. D. Bruce, W. Taylor, and A. F. Murray, J. Phys. C 13, 483 (1980).
[30]T. Schneider and E. Stoll, Ferroelectrics 12, 31 (1976); 24, 67 (1980).
[31]L. D. Landau and I. M. Khalatnikov, Dokl. Akad. Nauk SSSR 96, 469 (1959).
[32]W. Rehwald, Adv. Phys. 22, 721 (1973).
[33]K. Fossheim and B. Berre, Phys. Rev. B 5, 3292 (1972).